Axially Symmetric Model for Lattice Dynamics of Metals with Application to Cu, Al, and ZrH_2

G. W. LEHMAN, T. WOLFRAM, AND R. E. DE WAMES
North American Aviation Science Center, Conoga Park, California
(Received July 9, 1962)

A lattice dynamics model (A-S model) is proposed for metals which assumes that the restoring forces between the ions have the character of bond stretching and axially symmetric bond bending. It is shown that this type of restoring force is derivable from a sum of spherically symmetrical two-body potentials, $v(R_{ij})$, taken over all (i,j) pairs of lattice sites separated by a distance R_{ij}. The dynamical matrix for a face-centered cubic lattice is worked out for the first three neighbor shells of atoms. The dispersion curves for aluminum and copper are derived from the elastic constant and thermal diffuse x-ray data. The A-S force constants or Cu and Al fall off rapidly with distance and give dispersion curves which are at least as good as those derived from the third-neighbor general tensor force model. Particularly noteworthy is the fact that Walker's tensor force constants for Al are nearly axially symmetric. However, Jacobsen's tensor force constants for Cu are not axially symmetric. Contrary to this observation, it is found that White's force constants derived by using Feynman's theorem are nearly axially symmetric.

The A-S model is also applied to ZrH_2 which has a tetragonally deformed fluorite structure. It is shown that the six optical branches are flat to within 3% over the entire Brillouin zone and that the hydrogen-hydrogen interactions are very weak compared to the hydrogen-zirconium interactions. The dynamical matrix for the acoustic spectrum is derived.

I. INTRODUCTION

THIS paper is primarily concerned with the study of lattice vibrations in metals by using a model which is simpler than the tensor force model employed by Jacobsen[1] for copper and Walker[2] for aluminum. Our model is based upon the assumption that the internal energy of the system can be written as a sum of bond-stretching and bond-bending terms which have axial symmetry. We are able to relate the bond-bending force constants to the first derivatives of a two-body potential, v, and the bond-stretching force constants to the second derivatives of this same potential. We shall refer to our axially symmetric model as the A-S model for brevity. The tensor-force lattice dynamics model for a monatomic face-centered cubic crystal, employed by Jacobsen or Walker, requires nine atomic force constants in order to include contributions from the first three neighbors shells of atoms, while the A-S model requires only six.

In the case of aluminum, the force constants reported by Walker indicate axial symmetry. On the other hand, the force constants found by Jacobsen for copper are not axially symmetric. However, the experimental results have been fitted by a set of axially symmetric force constants which gives a better fit than Jacobsen obtained. Our force constants for copper bear a much closer relationship to those derived by White[3] from a first principle calculation.

A description of the A-S model is presented in Sec. II and is applied to aluminum and copper in Sec. III and the resulting dispersion curves are compared in Sec. IV with those obtained by Walker for aluminum and Jacobsen for copper by thermal diffuse x-ray analysis. White's results for copper are also included.

The vibration spectrum for ZrH_2 has also been examined using the A-S model and is described and compared with existing experimental results in Sec. V.

II. DESCRIPTION OF THE MODEL

The interaction potential between two atoms which have been displaced from equilibrium in a crystal is assumed to consist of two quadratic terms. The first is proportional to the square of the component of relative displacement along $\mathbf{R}$, the vector joining the equilibrium positions of the two atoms, and gives rise to a central or "bond-stretching" force. The second term is proportional to the square of the component of relative displacement perpendicular to $\mathbf{R}$ and causes a "bond-bending" force. Since all directions in the plane perpendicular to $\mathbf{R}$ are assumed equivalent, the interaction potential and corresponding forces are axially symmetric. It is important to note that our simple model can be derived from a sum of pair-wise interactions. If $v(|\mathbf{R}|)$ denotes the potential energy of interaction between two ions separated by a distance $|\mathbf{R}|$, then

$$v(|\mathbf{R}+\boldsymbol{\delta}|)=v(R)+v'(R)R^{-1}(\boldsymbol{\delta}\cdot\mathbf{R}) +\tfrac{1}{2}R^{-3}v'(R)(\boldsymbol{\delta}\times\mathbf{R})^2+1/2v''(R)R^{-2}(\boldsymbol{\delta}\cdot\mathbf{R})^2 +\text{higher terms in }\boldsymbol{\delta}, \quad (1)$$

where R is the magnitude of $\mathbf{R}$, $\boldsymbol{\delta}$ is an arbitrarily small vector displacement, and the primes on $v(R)$ denote differentiation with respect to R. The term linear in $\boldsymbol{\delta}$ in Eq. (1) must be taken into account when considering the static stability of a lattice but can be neglected in determining the lattice vibrational spectrum. The third and fourth terms in the above equation are the pair bond-bending and bond-stretching contributions which arise in molecular vibration theory.[4]

[1] E. H. Jacobsen, Phys. Rev. **97**, 654 (1955).
[2] C. B. Walker, Phys. Rev. **103**, 547 (1956).
[3] H. C. White, Phys. Rev. **112**, 1092 (1958).
[4] E. B. Wilson, J. C. Decius, and P. C. Cross, *Molecular Vibrations* (McGraw-Hill Book Company, Inc., New York, 1955).

Within the framework of the A-S model, one can write the quadratic terms in the potential energy of interaction associated with the αth atom in the zeroth unit cell as

$$V(0\alpha)=\tfrac{1}{2}\sum_\beta\sum_j|\mathbf{R}_j^{\alpha\beta}|^{-2}[C_1(j,\alpha\beta)(\mathbf{R}_j^{\alpha\beta}\cdot\Delta\mathbf{R}_j^{\alpha\beta})^2 +C_B(j,\alpha\beta)(\mathbf{R}_j^{\alpha\beta}\times\Delta\mathbf{R}_j^{\alpha\beta})^2]. \quad (2)$$

In this equation, $\mathbf{R}_j^{\alpha\beta}$ denotes a vector from the origin, chosen as the αth atom in the zeroth unit cell, to the βth atom in the jth cell. The Δ denotes a small displacement operator. $C_1(j,\alpha\beta)$ is the effective "bond-stretching" force constant for the interaction of the βth atom of the jth cell with the αth atom at the origin. Similarly, $C_B(j,\alpha\beta)$ represents an effective "bond-bending" force constant.

In the usual way,[5] one obtains the dynamical equations for the motion of the atoms in the central cell and introduces the usual Born-von Kármán cyclic boundary conditions. The vibrational spectrum is obtained by solving the determinant

$$|D(\mathbf{q})-\omega^2 I_{3f}|=0, \quad (3)$$

where ω is the angular frequency, $\mathbf{q}$ is the propagation vector, and I_{3f} denotes a unit matrix of dimension $3f$, with f being the number of atoms per unit cell. The dynamical matrix, D, may be conveniently regarded as an $f\times f$ supermatrix whose elements are 3×3 matrices. From Eq. (2), we obtain the $\alpha\beta$th element of the supermatrix, D, as

$$[D(\mathbf{q})]_{\alpha\beta}=(m_\alpha m_\beta)^{-1/2}(\delta_{\alpha\beta}\sum_{\sigma=1}^{f}A^{\alpha\sigma}(0)-A^{\alpha\beta}(\mathbf{q})), \quad (4)$$

where m_α is the mass of the αth type atom and $\delta_{\alpha\beta}$ is the Kronecker delta. The elements of the 3×3 matrices, $A^{\alpha\beta}(\mathbf{q})$, are given by

$$[A^{\alpha\beta}(\mathbf{q})]_{ij}=\sum_n\left(-|\mathbf{R}_n^{\alpha\beta}|^{-2}k_1(n,\alpha\beta)\frac{\partial^2}{\partial q_i\partial q_j} +C_B(n,\alpha\beta)\delta_{ij}\right)\exp(i\mathbf{q}\cdot\mathbf{R}_n^{\alpha\beta}), \quad (5)$$

where

$$k_1(n,\alpha\beta)=C_1(n,\alpha\beta)-C_B(n,\alpha\beta). \quad (6)$$

The subscripts on q_i in Eq. (5) refer to the Cartesian components of $\mathbf{q}$. Equation (5) can also be written as

$$[A^{\alpha\beta}(\mathbf{q})]_{ij}=\sum_s\left(-k_1(s,\alpha\beta)\rho_s^{-2}\frac{\partial^2}{\partial q_i\partial q_j} +C_B(s,\alpha\beta)\delta_{ij}\right)G(s,\alpha\beta), \quad (7)$$

where

$$\rho_s=|\mathbf{R}_{n(s)}^{\alpha\beta}| \quad (8)$$

is the distance between an α and a β atom in the sth shell about the α atom. In Eq. (7),

$$G(s,\alpha\beta)=\sum_{n(s)}\exp(i\mathbf{q}\cdot\mathbf{R}_n^{\alpha\beta}), \quad (9)$$

where the symbol $n(s)$ means that the sum is restricted to sth shell of atoms.

III. APPLICATION TO FACE-CENTERED CUBIC METALS

It is of considerable interest to apply our model to face-centered cubic aluminum and copper for which the results of the tensor force model are known.[1,2] The generators for the first three shells of neighbors for the face-centered cubic lattice with lattice constant $2a$ are

$$\begin{aligned}G(1)&=4(C_xC_y+C_yC_z+C_zC_x),\\ G(2)&=2(C_{2x}+C_{2y}+C_{2z}),\\ G(3)&=8(C_{2x}C_yC_z+C_xC_{2y}C_z+C_xC_yC_{2z}),\end{aligned} \quad (10)$$

where

$$C_{np}=\cos(nq_pa), \quad p=x,\ y,\ \text{or}\ z. \quad (11)$$

For sake of completeness, we list the dynamical matrix elements derived by use of Eqs. (4)–(9). The diagonal elements of D are given by

$$\begin{aligned}MD_{ii}=&4C_B(1)[3-C_iC_j-C_jC_k-C_kC_i]\\ &+2C_B(2)[3-C_{2i}-C_{2j}-C_{2k}]\\ &+8C_B(3)[3-C_{2i}C_jC_k-C_{2j}C_kC_i-C_{2k}C_iC_j]\\ &+2k_1(1)[2-C_i(C_j+C_k)]+2k_1(2)[1-C_{2i}]\\ &+\tfrac{4}{3}k_1(3)[6-4C_{2i}C_jC_k\\ &\qquad-C_i(C_{2j}C_k+C_{2k}C_j)].\end{aligned} \quad (12)$$

Similarly, the off-diagonal elements of D are given by

$$\begin{aligned}MD_{ij}=&2k_1(1)S_iS_j\\ &+\tfrac{4}{3}k_1(3)[S_iS_jC_{2k}+2C_k(S_{2i}S_j+S_{2j}S_i)].\end{aligned} \quad (13)$$

In the above equations, i, j, and k stand for x, y, and z. M is the mass of the atom and the S_i's stand for the sine functions whose arguments are the same as those appearing in Eq. (11).

A correlation between the tensor force and A-S model shows that the tensor force constants α_i, β_i, and γ_i defined by Walker for a face-centered cubic lattice are related to the A-S force constants as shown below.

$$\begin{aligned}\alpha_1&=C_B(1)+\tfrac{1}{2}k_1(1)\\ \beta_1&=C_B(1)\\ \gamma_1&=\alpha_1-\beta_1=\tfrac{1}{2}k_1(1),\\ \alpha_2&=C_B(2)+k_1(2),\\ \beta_2&=C_B(2),\\ \alpha_3&=C_B(3)+\tfrac{2}{3}k_1(3),\\ \beta_3&=C_B(3)+\tfrac{1}{6}k_1(3),\\ \gamma_3&=\alpha_3-\beta_3=\tfrac{1}{6}k_1(3),\\ \delta_3&=\tfrac{1}{3}k_1(3).\end{aligned} \quad (14)$$

[5] For a recent review article on lattice dynamics see J. Krumhansl, Suppl. J. Appl. Phys. **33**, 307 (1962). See also M. Born and K. Huang, *Dynamical Theory of Crystal Lattices* (Oxford University Press, New York, 1954).

A. Relationship between Elastic Constants and A-S Force Constants

Relationships between the elastic constants and the A-S force constants are derived by going to the long-wavelength limit.[6] One finds that

$$C_B(1)+C_B(2)+6C_B(3)=\tfrac{1}{4}a(2c_{44}-c_{12}-c_{44}),$$
$$k_1(2)=\tfrac{1}{4}a(2c_{11}-c_{12}-3c_{44}), \quad (15)$$
$$k_1(1)+6k_1(3)=a(c_{12}+c_{44}).$$

These equations indicate that $k_1(2)$ is fixed uniquely in terms of the elastic constants.

B. Dispersion Curves along the Principal Axes

The dispersion curves are easily obtained along the [100], [110], and [111] directions in **q** space. The results are presented below.

[100] Direction

$$\omega_L^2=D_{xx}(100),$$
$$\omega_T^2=D_{yy}(100). \quad (16)$$

[110] Direction

$$\omega_L^2=D_{xx}(110)+D_{xy}(110),$$
$$\omega_{T_1}^2=D_{xx}(110)-D_{xy}(110), \quad (17)$$
$$\omega_{T_2}^2=D_{zz}(110).$$

[111] Direction

$$\omega_L^2=D_{xx}(111)+2D_{xy}(111),$$
$$\omega_T^2=D_{xx}(111)-D_{xy}(111). \quad (18)$$

In the above equations, $D_{ij}(pqr)$ are determined along the $[pqr]$ direction in **q** space from Eqs. (12) and (13). The subscripts L and T refer to longitudinal and transverse modes where the transverse modes are doubly degenerate along the [100] and [111] directions.

IV. DISPERSION CURVES FOR ALUMINUM AND COPPER

For a third nearest neighbor calculation, the A-S model requires the determination of six atomic force constants while the tensor force model requires nine constants. These A-S parameters were determined for aluminum and copper according to a very simple procedure. First, the three elastic equations [see Eq. (15)] were imposed as constraining equations. This insured that the dispersion curves would have the correct slope in the region of small **q**. In order to fix the high-frequency end of the spectrum, three data points near the edge of the Brillouin zone were selected. Since there are seven distinct branches of the dispersion curves along the three symmetry directions, these three points could be selected in a variety of ways. The eigenfrequencies of the dynamical matrix were then required to match these selected points. This gives three additional equations so that the force constants are uniquely determined for a particular set of points. By selecting different sets of data points, a number of sets of force constants were obtained. The results of this analysis indicate all sets of force constants are almost identical and our final set was obtained by a simple averaging process.

[6] For this derivation, see A. E. H. Love, *Mathematical Theory of Elasticity* (Dover Publications, New York, 1944).

TABLE I. A–S force constants for aluminum and copper (in units of 10^{3} dyn/cm).

Aluminum	Copper
$k_1(1)=18.7$	$k_1(1)=22.50$
$C_B(1)=-0.9$	$C_B(1)=-0.01$
$k_1(2)=3.0$	$k_1(2)=-0.12$
$C_B(2)=-1.0$	$C_B(2)=-0.11$
$k_1(3)=0.0$	$k_1(3)=0.22$
$C_B(3)=0.0$	$C_B(3)=-0.03$

A. Comparison of the A-S Results with Experiment

Aluminum

The results of this study for aluminum are summarized in Table I. The dispersion curves calculated from these values are shown in Figs. 1–3, where they may be compared with the experimental data and the theoretical curves of Walker. The agreement with experiment is obviously quite good. It is worth pointing out that since the third-neighbor interactions vanish we have effectively only one parameter in the A-S model (the other three constants being determined by the elastic equations). Nevertheless, the fit obtained with this single parameter is equivalent to that obtained by

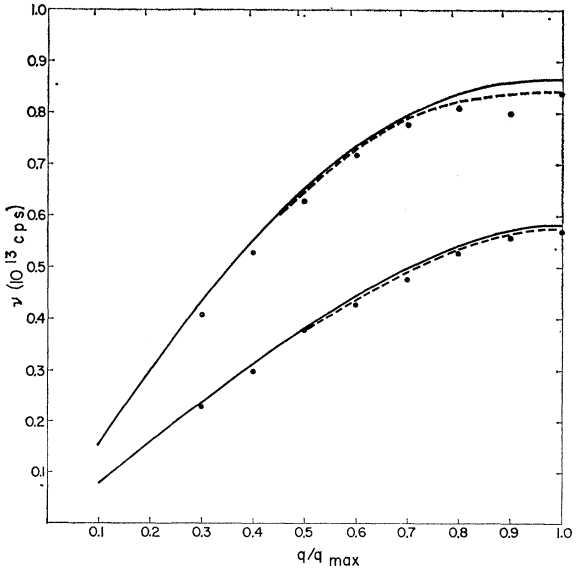

FIG. 1. Dispersion curves for aluminum along [100] direction in Brillouin zone. Solid circles denote Walker's data. Dashed lines denote tensor force model. Solid lines refer to A-S model.

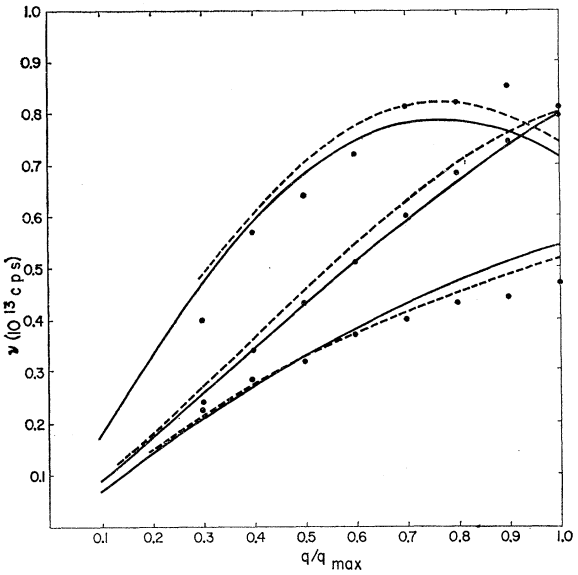

FIG. 2. Dispersion curves for aluminum along [110] direction in Brillouin zone. See Fig. 1 for labeling of curves.

Walker using 9 force constants. In addition, we obtain the elastic constants exactly. The results are also encouraging inasmuch as there is a rapid convergence of the force constants. In Table II, the force constants of Walker and the corresponding tensor force constants from the A-S model calculated by means of the correlation equations [Eq. (14)] are compared. It is seen that Walker's first-neighbor force constants are essentially axially symmetric.

Copper

The A-S force constants derived from the experimental data by Jacobsen[1] for copper are also summarized in Table I. The corresponding dispersion curves are shown in Figs. 4–6. In our opinion the A-S dispersion curves give a better over-all fit to the experimental data than the theoretical curves of Jacobsen. It is interesting that the tensor force constants computed from the A-S force model bear no resemblance to those calculated by Jacobsen. In Table III, we have also listed the tensor force constants computed by White[3] from what amounts to a first principles calculation using Feynman's theorem. There is a good deal of correlation between White's atomic force constants and those obtained from the axially symmetric force constant model.

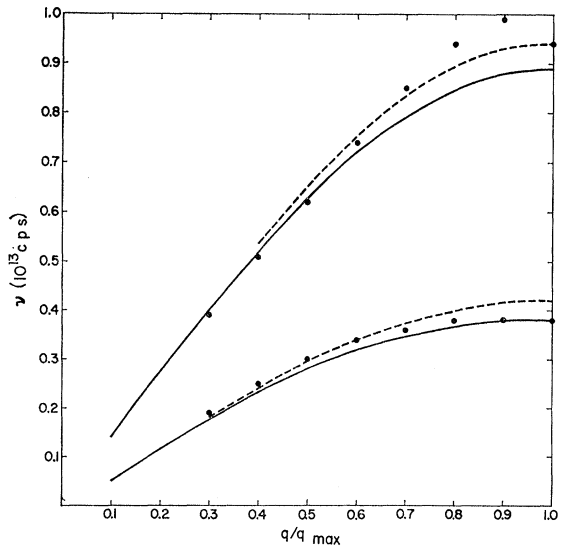

FIG. 3. Dispersion curves for aluminum along [111] direction in Brillouin zone. See Fig. 1 for labeling of curves.

V. APPLICATION TO ZIRCONIUM HYDRIDE

The vibrational spectrum of the ϵ phase of zirconium hydride, ZrH_2, will be worked out in this section using the A-S model. This hydride has a tetragonally distorted fluorite structure with three atoms per unit cell. The lattice constants reported by Flotow and Osborne[7] are $a_0=4.98\pm0.01$ Å and $c_0=4.45\pm0.01$ Å for a face-centered tetragonal lattice.

TABLE II Atomic force constants for aluminum (in units of 10^3 dyn/cm^{-1})

Force constant		Walker's value	A-S value
1	α_1	8.45	8.45
2	β_1	−0.93	−0.9
3	γ_1	10.67	9.35
4	α_2	2.14	2.0
5	β_2	0.40	−1.0
6	α_3	0.27	0
7	β_3	−0.31	0
8	γ_3	0.10	0
9	δ_3	−0.19	0

Experimental evidence, based on inelastic neutron scattering[8] and heat capacity measurements,[7] shows that the optical frequencies of ZrH_2 are nearly sixfold degenerate with a wave number of 1190 ± 30 cm^{-1}.

Dynamical Matrix for ZrH_2

The dynamical matrix for ZrH_2, based on the A-S model, can be written as

$$D=\begin{bmatrix} B_{11} & B_{12} & B_{12}^* \\ B_{12}^* & B_{22} & B_{23} \\ B_{12} & B_{23} & B_{22} \end{bmatrix}. \tag{19}$$

The 3×3 B_{ij}^* matrices refer to the complex conjugate transpose of B_{ij}. The subscripts 1, 2, and 3 refer to the three face-centered tetragonal lattices composed of zirconium, hydrogen, and hydrogen, respectively. The hydrogen lattices are based on $(\frac{1}{4}a_0,\frac{1}{4}a_0,\frac{1}{4}c_0)$ and $(\frac{3}{4}a_0,\frac{1}{4}a_0,\frac{1}{4}c_0)$ relative to the zirconium lattice at (0,0,0).

[7] H. E. Flotow and D. W. Osborne, J. Chem. Phys. **34**, 1418 (1961).
[8] W. L. Whittemore and A. W. McReynolds, Phys. Rev. **113**, 806 (1959).

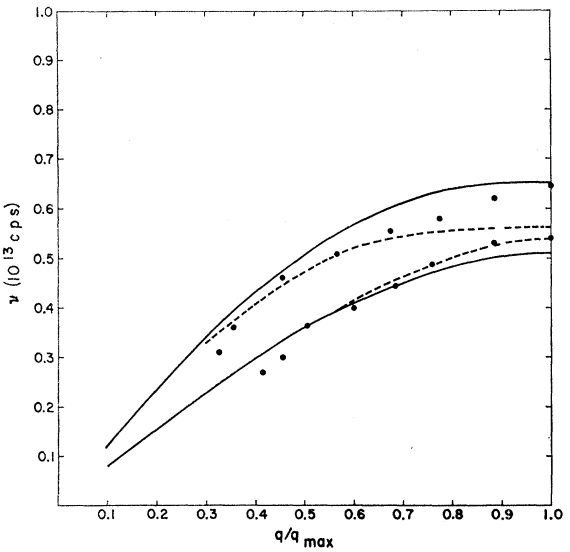

FIG. 4. Dispersion curves for copper along [100] direction in Brillouin zone. Solid circles denote Jacobsen's data. Dashed and solid lines refer to tensor and A-S model, respectively.

From Eq. (4), one notes that

$$\begin{aligned} B_{11}&=(m_1)^{-1}[A_{11}(0)+2A_{12}(0)-A_{11}(\mathbf{q})],\\ B_{12}&=-(m_1m_2)^{-1/2}A_{12}(\mathbf{q}),\\ B_{22}&=(m_2)^{-1}[A_{12}(0)+A_{22}(0)+A_{23}(0)-A_{22}(\mathbf{q})],\\ B_{23}&=-(m_2)^{-1}A_{23}(\mathbf{q}). \end{aligned} \tag{20}$$

Transformation of Dynamical Matrix to Real Form

The dynamical matrix, Eq. (19), can be transformed by a unitary transformation, U, into a real-symmetric matrix, D', since the dynamical equations possess time-reversal symmetry and the lattice possesses inversional symmetry. An examination of Eq. (19) shows that

$$U=\begin{bmatrix} I_3 & O_3 & O_3 \\ O_3 & 2^{-1/2}I_3 & i2^{-1/2}I_3 \\ O_3 & 2^{-1/2}I_3 & -2^{-1/2}iI_3 \end{bmatrix}, \tag{21}$$

where I_3 and O_3 refer to 3×3 identity and null matrices, respectively. It follows that the transformed dynamical matrix is

$$D'=U^*DU=\begin{bmatrix} B_{11} & 2^{1/2}\,\mathrm{Re}(B_{12}) & 2^{1/2}\,\mathrm{Im}(B_{12}) \\ 2^{1/2}\,\mathrm{Re}(B_{12}) & B_{22}+B_{23} & O_3 \\ 2^{1/2}\,\mathrm{Im}(B_{12}) & O_3 & B_{22}-B_{23} \end{bmatrix}, \tag{22}$$

where Re and Im refer to real and imaginary parts of B_{12}.

TABLE III. Atomic force constants for copper (in units of 10^4 dyn/cm^{-1}).

	Jacobsen	White	A-S
α_1	0.87	1.71	1.21
β_1	0.48	−0.24	−0.001
γ_1	1.25	1.66	1.124
α_2	0.35	−0.13	−0.0227
β_2	−0.072	−0.07	0.0105
α_3	0.09	−0.01	0.1122
β_3	−0.022	+0.005	0.00345
γ_3	−0.015	+0.02	0.03625
δ_3	0.06	+0.01	0.0725

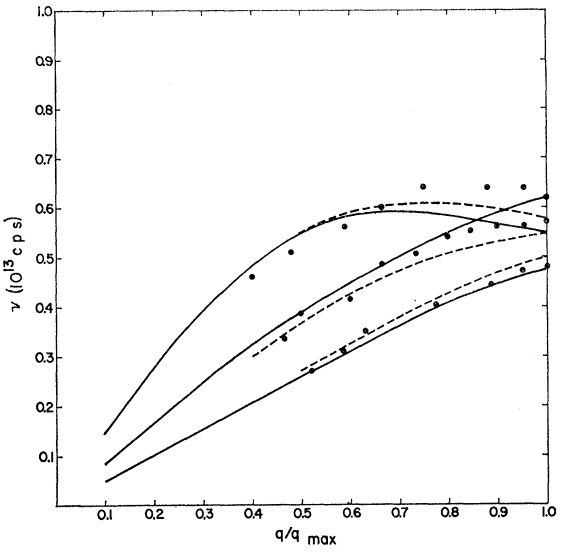

FIG. 5. Dispersion curves for copper along [110] direction in Brillouin zone. See Fig. 4 for labeling of curves.

Dynamical Matrix in Long-Wavelength Limit

Experimental evidence cited at the beginning of this section suggests that the optical and acoustical modes are separated by a large frequency range. At $\mathbf{q}=0$, one

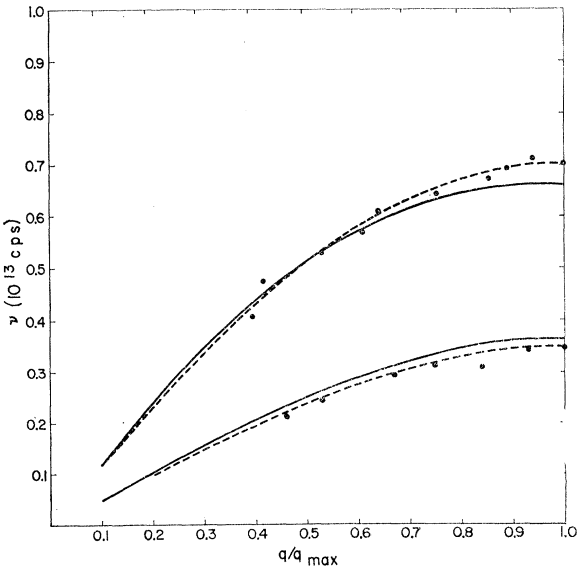

FIG. 6. Dispersion curves for copper along [111] direction in Brillouin zone. See Fig. 4 for labeling of curves.

can show by group-theoretical arguments that there are three zero frequencies, two sets of doubly degenerate frequencies, and two sets of nondegenerate frequencies. Consequently, the D' matrix can be block diagonalized by a unitary transformation, U_0, for $\mathbf{q}=0$ with the largest blocks consisting of 2×2 matrices. The transformation which accomplishes this is associated with the introduction of center-of-mass coordinates. We find that

$$U_0=\frac{1}{(2m_2+m_1)^{1/2}}\begin{pmatrix}(2m_2)^{1/2}I_3 & -(m_1)^{1/2}I_3 & O_3\\ (m_1)^{1/2}I_3 & (2m_2)^{1/2}I_3 & O_3\\ O_3 & O_3 & \sigma I_3\end{pmatrix}, \quad (23)$$

where $\sigma=(2m_2+m_1)^{1/2}$.

This transformation also separates the acoustical and optical modes in the long-wavelength region and will yield directly the proper limiting form of the dynamical acoustic matrix for small $\mathbf{q}$. From Eqs. (20), (22), and (23) one can show that

$$D''=U_0{}^*D'U_0=\begin{pmatrix}gA_{12}(0) & O_3 & O_3\\ O_3 & W_a & O_3\\ O_3 & O_3 & m_2{}^{-1}[A_{12}(0)+2A_{23}(0)]\end{pmatrix}, \quad (24)$$

where

$$g=(2m_2+m_1)/m_1m_2. \quad (25)$$

In Eq. (24),

$$W_a=[1/(2m_2+m_1)][\Delta A_{11}(\mathbf{q})+4\,\mathrm{Re}(\Delta A_{12}(\mathbf{q})+2\Delta A_{22}(\mathbf{q})+2\Delta A_{23}(\mathbf{q})] \quad (26)$$

represents the dynamical acoustical matrix for small $\mathbf{q}$ where

$$\Delta A_{ij}=A_{ij}(0)-A_{ij}(\mathbf{q}). \quad (27)$$

Characterization of the Optical Modes

From Eqs. (7) and (9) one finds that

$$A_{\alpha\beta}(0)=\begin{pmatrix}K_{\alpha\beta;x} & 0 & 0\\ 0 & K_{\alpha\beta;x} & 0\\ 0 & 0 & K_{\alpha\beta;z}\end{pmatrix}, \quad (28)$$

where

$$K_{\alpha\beta;T}=\sum_s k_1(s,\alpha\beta)\rho_s{}^{-2}\sum_n (T_n{}^{\alpha\beta})^2+\sum_s N(s)C_2(s,\alpha\beta). \quad (29)$$

In Eq. (29), T stands for x or z and $N(s)$ represents the number of β neighbors in the sth shell about an αth site.

From Eqs. (24) and (28), it follows that the optical angular frequencies at $\mathbf{q}=0$ are

$$\begin{aligned}\omega_{1,2}&=[(2m_2+m_1)/m_1m_2]^{1/2}(K_{12;x})^{1/2},\\ \omega_3&=[(2m_2+m_1)/m_1m_2]^{1/2}(K_{12;z})^{1/2},\\ \omega_{4,5}&=(m_2)^{-1/2}(K_{12;x}+2K_{23;x})^{1/2},\\ \omega_6&=(m_2)^{-1/2}(K_{12;z}+2K_{23;z})^{1/2}.\end{aligned} \quad (30)$$

Since $m_1/m_2=91.2$ and 45.6 for ZrH_2 and ZrD_2, respectively, one notes that the frequencies are inversely proportional to $(m_2)^{1/2}$ to within 1 or 2%. Furthermore, the experimental evidence,[7] cited previously, shows that no more than $\pm3\%$ spread exists in the frequencies. Consequently, the expressions for $\omega_{1,2}$ and ω_3 show that $K_{12;x}$ cannot deviate from $K_{12;z}$ by more than about $\pm6\%$. Similar conclusions must hold for the last two equations of Eq. (30). We also note from a comparison of $\omega_{1,2}$ and $\omega_{4,5}$ or ω_3 and ω_6 that $K_{23;x}$ cannot be greater than ±4 or 5% of $K_{12;x}$.

The six optical frequency branches have been examined in some detail at all points in the zone and we find that these branches are flat to within a few percent. Our final conclusion, based upon our lattice dynamics study and the available experimental data, is that the hydrogen-hydrogen interactions are quite weak compared to the hydrogen-zirconium interactions.

The Acoustical Modes in ZrH_2

We wish to point out that Eq. (26) for W_a represents a good approximation to the dynamical acoustical matrix over the entire zone. The coupling between acoustical and optical modes is quite weak and preliminary calculations indicate that a maximum error of about 3% is introduced in the acoustical spectrum by neglecting the optical-acoustical coupling. In this mode of vibration, all three lattices move in phase. From the form of Eq. (26), we note that the hydrogen-zirconium coupling plays a vital role in determining the acoustical vibration spectrum. One also notes that the effective mass associated with the acoustic modes is simply m_1+2m_2, the factor of 2 coming from the two hydrogen lattices.

VI. SUMMARY AND CONCLUSIONS

A simple lattice dynamics model for metals has been developed in this paper which is based upon the assumption that the total energy, E, of the system can be written as

$$E=E_0+\sum_i\sum_{i>j} v(R_{ij}),$$

where $v(R_{ij})$ is a potential energy function which specifies the effective interaction between the ith and jth ion separated by a distance R_{ij}. Here, E_0 is an energy which is independent of the relative separation of the ions. We have shown that our A-S model can be characterized by the well-known bond-stretching and axially symmetric bond-bending interactions used in molecular vibration theory.

We obtain excellent agreement with the dispersion curves obtained from thermal diffuse x-ray scattering data of Walker on aluminum and Jacobsen on copper by using the first-, second-, and third-neighbor interactions. We require that the dispersion curves have the correct behavior in the long-wavelength or elastic constant limit. In both copper and aluminum, the A-S

force constants were found to fall off quite rapidly. This behavior indicates that the potential energy interaction function, $v(R_{ij})$, has a well-defined minimum at the nearest-neighbor separation and decreases rapidly and has an oscillatory behavior at the second- and third-neighbor positions. These conclusions are consistent with the theoretical analyses of Langer and Vosko[9] which strongly suggest that the interaction potential between a pair of ions in an electron gas would have an oscillatory behavior as a function of separation distance.

A second application of the A-S model has been carried out on zirconium hydride and deuteride which have tetragonally deformed fluorite structures. We have concluded from this study that the hydrogen-hydrogen interaction is very weak compared to the hydrogen-zirconium interaction and that the six optical branches are nearly degenerate and have frequencies which are independent of the propagation vector to within 3%.

[9] J. S. Langer and S. H. Vosko, J. Phys. Chem. Solids **12**, 196 (1959).

PHYSICAL REVIEW VOLUME 128, NUMBER 4 NOVEMBER 15, 1962

Magnetization of Slow Electrons in a Polar Crystal

R. W. HELLWARTH
Hughes Research Laboratories, Malibu, California

P. M. PLATZMAN
Bell Telephone Laboratories, Murray Hill, New Jersey

(Received April 23, 1962)

An approximate expression for the free energy of an electron which is coupled to a phonon field (a "polaron") and is in a uniform magnetic field is given. This expression is obtained by an extension of Feynman's path integral variational calculation of the polaron binding energy and is valid for all values of the field, the temperature and the electron-lattice coupling strength. The explicit form of the result is given in terms of a model system with an action functional different from that of the actual problem. A minimum-variational method is given for determining the best model to employ in calculations. We have evaluated the magnetic free energy at small magnetic fields using a model of a simple form. The two variable parameters of this model have already been optimized by Feynman and Schultz for Fröhlich's Hamiltonian and zero field. The result is applicable at all coupling strengths and carried to the first two terms in a Laurent series in the temperature. The first (inverse temperature) term yields an approximation to the effective polaron mass that varies, as the coupling is varied, by at most 1.5% from that calculated by Feynman and others. The second (temperature independent) term reflects the internal structure (atomic diamagnetism) of the polaron at large coupling and also the temperature variation of effective mass. The difference between our magnetic mass and that calculated by Feynman is shown to disappear when the model system is fully optimized.

I. FORMULATION AND METHOD OF APPROXIMATION

AN electron in the interior of an ionic crystal surrounds itself with a distorted lattice; a cloud of phonons. This system, commonly called a polaron, has been extensively studied theoretically.[1–6] We present here a calculation for the free energy of this coupled electron-phonon system in a uniform magnetic field. The results are obtained by an extension of Feynman's variational calculation of the polaron binding energy[7] and are applicable at all values of the magnetic field, the temperature and the electron-lattice coupling strength. The susceptibility χ and other quantities of interest are easily obtainable from the free energy F. We will not attempt here to assess all those effects that would be present in a real material,[4] but rather treat the polaron as an idealized mathematical model. For numerical computations, we will specialize even further and use the Fröhlich model of the polaron[2] in order to compare our results with those of other theories.

To obtain the polaron free energy F as a function of the applied uniform magnetic field H (taken to be in the z direction), we use a path integral formulation equivalent to the $\mathrm{Tr}[\exp(-\beta\mathfrak{IC})]$. This allows the elimination of all phonon coordinates from the expression for F and results in an expression of the form.[1,8]

$$e^{-\beta F}=\sum_{\mathbf{X}(t)}\exp\{S[\mathbf{X}(t)]\}. \tag{1}$$

The symbol $\sum_{\mathbf{X}(t)}$ denotes the "path integral," or sum over all electron trajectories $\mathbf{X}(t)$ for t in the domain 0

[1] R. P. Feynman, Phys Rev. **97**, 660 (1955); hereafter to be called I.
[2] H. Fröhlich, in *Advances in Physics*, edited by N. F. Mott (Taylor and Francis, Ltd., London, 1954), Vol. 3, p. 325.
[3] S. I. Pekar, Zhur. Eksp. i Teoret. Fiz. **19**, 796 (1949).
[4] T. D. Schultz, Phys. Rev. **116**, 526 (1960). References 2–4 contain a more complete bibliography of polaron studies.
[5] P. M. Platzman, Phys. Rev. **125**, 1961 (1962).
[6] M. Krivoglaz and S. I. Pekar, Izvest. Akad. Nauk S.S.S.R. Ser. Fiz. **21**, 1, 16, 33 (1957).
[7] Y. Osaka, Progr. Theoret. Phys. Japan **22**, 437 (1959).
[8] R. P. Feynman, Phys. Rev. **84**, 108 (1951).